Accepted Manuscript

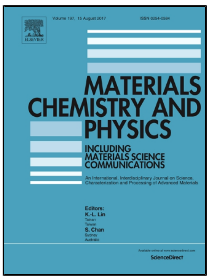

Surface modification after ethanol wet milling: A comparison between pristine glasses produced from natural minerals and analytical grade raw materials

Franco Matías Stábile, Elena Rodríguez-Aguado, Enrique Rodríguez-Castellón, Cristina Volzone

PII:	S0254-0584(17)30515-1
DOI:	10.1016/j.matchemphys.2017.07.006
Reference:	MAC 19813
To appear in:	*Materials Chemistry and Physics*
Received Date:	18 November 2016
Revised Date:	06 May 2017
Accepted Date:	02 July 2017

Please cite this article as: Franco Matías Stábile, Elena Rodríguez-Aguado, Enrique Rodríguez-Castellón, Cristina Volzone, Surface modification after ethanol wet milling: A comparison between pristine glasses produced from natural minerals and analytical grade raw materials, *Materials Chemistry and Physics* (2017), doi: 10.1016/j.matchemphys.2017.07.006

Surface modification after ethanol wet milling: A comparison between pristine glasses produced from natural minerals and analytical grade raw materials.

Franco Matías Stábile[1]*, Elena Rodríguez-Aguado[2], Enrique Rodríguez-Castellón[2], Cristina Volzone[1*].

[1] Centro de Tecnología de Recursos Minerales y Cerámica (CETMIC), CONICET CCT La Plata-CICPBA. Camino Centenario y 506, M.B. Gonnet, C.P.1897, Province of Buenos Aires, Argentina.

[2] Departamento de Química Inorgánica, Facultad de Ciencias, Universidad de Málaga, 29071 Málaga, Spain.

Abstract

Four glass compositions were produced taking into account different theoretical Leucite ($KAlSi_2O_6$)/Bioglass 45S5 (45 % SiO_2, 24.5 % Na_2O, 24.5 % CaO, 6 % P_2O_5) ratios using analytical grade reagents only; and replacing some of the reagents by natural minerals, all that were found to be bioactive when they were transformed to glass ceramics. Glasses of particle size below 174 μm were wet milled using ethanol in a high energy planetary ball mill. After wet milling, samples with 25 and 30 % of theoretical Leucite content using reagents grade raw materials showed a higher dissolution rate in comparison to the same glasses made from natural mineral, while no differences were found on glasses with 40 and 50 % of Leucite theoretical content. Samples with higher dissolution showed a crystalline carbonate phase named Pirssonite on its surface, while on the rest of samples amorphous carbonates were present.

Keywords: Glass surface, bioactive glass, wet milling, XPS, FTIR.

Introduction

Bioglass 45S5 is well known for being one of the most important bioactive glasses, and it is widely used in clinical applications [1]. In the last few years, efforts have been made to impart bioactivity to dental glass-ceramics. The induction of bioactivity on glass-ceramics with dental applications has been achieved through dental glass-ceramics/bioactive glass composites (eg. 45S5, 58S) [2, 3]; as well as through pristine glasses of different compositions, that were calculated in the basis of different theoretical weight ratios of Leucite ($KAlSi_2O_6$) and Bioglass 45S5 [4], which were also produced using natural minerals.

Grinding of pristine glass to a small particle size is a relevant processing stage for Leucite surface crystallization [5, 6]. At the same time, it is usual that these types of materials are produced from analytical grade reagents; although it would be possible to incorporate natural raw materials by controlling their degree of purity [7].

There are scarce studies related to the influence of milling conditions [8, 9] and no similar works related to the influence of raw materials origin on glass changes before glass-ceramics production have been found to the best of our knowledge. It would be interesting to study the influence of a high energy wet milling; a necessary process to achieve a particle size suitable for the processing of Leucite glass-ceramics, so as to know the relevant structural changes that occur in glass during this stage. At the same time, a study of interest would be to compare the possible differences in the properties and characteristics of the glasses produced from pure reagents with respect to those obtained from minerals. This study will provide detailed knowledge of all the processes involved in the preparation of the final product.

The objective of this study was to evaluate the possible structural and surface differences between glasses with the same composition but made from natural raw

materials and analytical grade reagents, as well as the influence of wet and dry milling with respect to the used raw materials.

Materials and methods

Four glass compositions were made on the basis of different theoretical Leucite/Bioglass 45S5 ratios, being 25/75, 30/70, 40/60 and 50/50 (wt. %). Each composition was prepared using analytical grade reagents only, and the same compositions were also produced by replacing some of the reagents by natural minerals. Reagent grade raw materials were sodium carbonate (Anedra), calcium carbonate (Anedra), ammonium dihydrogen phosphate (Anedra), aluminum hydroxide (Anedra), potassium carbonate (Biopack) and amorphous silica (Carlo Erba), each of one incorporating its respective oxide only to the glass composition. Natural minerals were high purity quartz and potassium feldspar provided by a Argentinian mining company. Table 1 shows the chemical analyses of the natural raw materials. In this way, aluminum hydroxide, amorphous silica, almost 70 % of potassium carbonate, and a minimum quantity of calcium carbonate and sodium carbonate were replaced for feldspar and quartz to reproduce each composition (Table 2).

Table 1. Chemical analyses of natural raw materials

Raw Material	SiO_2	Al_2O_3	Na_2O	K_2O	CaO	Fe_2O_3	TiO_2
Feldspar	66.25	18.42	2.06	12.02	0.20	0.05	0.01
Quartz	99.33	0.49	0.06	0.10	0.00	0.01	0.00

Replacements were made in function of minerals compositions.

Table 2. Mineral and reagent grade raw materials contributions to glasses compositions.

Samples	Feldspar %	Quartz %	Aluminum Hydroxide (as Aluminum Oxide) %	Amorphous Silica %	Potassium Carbonate (as Potassium Oxide) %	Ammonium Dihydrogen Phosphate (as Phosphorus Pentoxide) %	Sodium Carbonate (as Sodium Oxide) %	Calcium Carbonate (as Calcium Oxide) %
L25 M	30.71	27.13	-------	-------	1.64	4.50	17.72	18.30
L30 M	37.09	23.33	-------	-------	1.95	4.20	16.36	17.06
L40 M	49.86	15.74	-------	-------	2.57	3.60	13.65	14.58
L50 M	62.63	8.15	-------	-------	3.19	3.00	10.94	12.10
L25 R	-------	-------	5.84	47.59	5.38	4.50	18.35	18.35
L30 R	-------	-------	7.00	48.09	6.46	4.20	17.12	17.12
L40 R	-------	-------	9.34	49.09	8.61	3.60	14.68	14.68
L50 R	-------	-------	11.67	50.10	10.77	3.00	12.23	12.23

Table 3. Glasses compositions and identifications. Suffixes (c) and (f) correspond to coarse and fine, respectively. (L: Leucite; R: Reagents; M: Minerals reagents)

	Compositions (wt.%)				
Raw Materials	*Leucite*	*25*	*30*	*40*	*50*
	Bioglass	*75*	*70*	*60*	*50*
Reagents	Dry milled	L25 Rc	L30 Rc	L40 Rc	L50 Rc
	Wet milled	L25 Rf	L30 Rf	L40 Rf	L50 Rf
Minerals + Reagents	Dry milled	L25 Mc	L30 Mc	L40 Mc	L50 Mc
	Wet milled	L25 Mf	L30 Mf	L40 Mf	L50 Mf

The mixtures were heat treated at 900 °C for decarbonation, fused at 1350°C for 1 hour in a platinum crucible and cast into water to make glass frits. The obtained glasses were dry milled into a porcelain mortar up to reach a maximum particle size of 149 µm

(100 mesh sieve) and identify as coarse (c). Half of the sieved glass was wet milled using 96% ethanol as milling media and identify as fine (f). Glasses identifications are shown in Table 3. The glasses were milled in a high energy planetary ball mill Pulverisette 7 at 500 rpm using 60 milling cycles of 1 minute. Once the milling was finished, ethanol was dried at ambient temperature in air.

Particle size distribution of both glass fractions (coarse and fine) of each glass made from different raw materials were measured by means of a Malvern Mastersizer 2000 equipment, with Hydro 2000 G dispersion unit and water as a dispersant.

All fine and coarse glasses were characterized by X-ray diffraction (XRD), using a Phillips 3010 diffractometer with Cu Kα radiation and Ni filter. Diffractograms were acquired in a 2θ range between 10 and 70 °, 0.04 ° step and 2 seconds per step.

Bulk chemical analyses of the coarse glasses were carried out by X-ray fluorescence in a Shimadzu EDX 800 HS equipment.

Fourier transformed infrared (FTIR) spectra (4000–400 cm^{-1}) of glasses were measured by means of a Thermo Nicolet 6700 equipment. Each spectrum was taken using 2 cm^{-1} step with aperture of 100 and 32 scans. The samples were dispersed in KBr (1 wt.%) and compacted in a thin pellet form. Spectra were plotted in transmittance mode.

Surface chemical characterization was carried out by X-Ray Photoelectron Spectroscopy (XPS) using a Physical Electronics PHI 5700 spectrometer with non-monochromatic Mg-Kα radiation (300 W, 15 kV, 1253.6 eV) as the excitation source. High-resolution spectra of C 1*s*, O 1*s*, Na 1*s*, Al 2*p*, Al KLL, Si 2*p*, P 2*p* and K 2*p*, were recorded at 45° take-off-angle by a concentric hemispherical analyzer operating in the constant pass energy mode at 29.35 eV, using a 720 μm diameter analysis area. Under these conditions the Au $4f_{7/2}$ line was recorded with 1.16 eV full width at half-maximum (FWHM) at a binding energy (BE) of 84.0 eV., binding energy values were referenced to the C 1*s* peak (284.8 eV) from the adventitious contamination layer. The

PHI Access ESCA-V6.0 F and Multipak software packages were used for acquisition and data analysis. Atomic concentration percentages of the studied elements were determined after subtraction of a Shirley-type background, taking into account the corresponding area sensitivity factor [10] for the different measured spectral regions. Recorded spectra were always fitted using Gauss-Lorentz curves, in order to determine the binding energy of the different element core levels more accurately. The error in BE was estimated to be *ca*. 0.1 eV.

Results and discussion

Mean particle size

The mean particle sizes of all samples are shown in table 4.

Table 4. Particle sizes distribution of coarse (c) and fine (f) fractions of each glass composition made from reagent grade (R) and mineral (M) raw materials.

Samples	Mean particle size (µm)			Samples	Mean particle size (µm)		
	d 0.1	d 0.5	d 0.9		d 0.1	d 0.5	d 0.9
L25 Mg	2.98	10.02	55.21	L25 Rg	2.78	10.66	59.76
L25 Mf	2.46	5.53	11.97	L25 Rf	2.16	4.73	9.66
L30 Mg	2.75	11.20	58.02	L30 Rg	2.29	9.51	56.32
L30 Mf	2.00	4.98	10.84	L30 Rf	1.77	5.04	11.47
L40 Mg	2.53	9.98	57.90	L40 Rg	4.12	9.87	60.12
L40 Mf	1.98	5.33	12.01	L40 Rf	3.91	8.70	17.54
L50 Mg	3.01	10.54	60.41	L50 Rg	2.85	10.24	64.48
L50 Mf	1.90	4.54	9.67	L50 Rf	2.77	6.35	13.41

X-Ray Diffraction

X-ray diffractograms of all studied glasses showed remarkable differences as a function of compositions and after the wet milling process (Figures 1-4). Samples grinded at high energy with ethanol (samples Rf) showed a higher amount of a crystalline phase. This fact is ascribed to the phase Pirssonite, ($Na_2Ca(CO_3)_2$ $2H_2O$),(diffraction peaks at:17.37, 18.01, 28.22, 31.00, 33.79, 34.88, 35.89, 44.83, 51.59 °2θ) whereas diffraction patterns of dry milled samples showed no diffraction lines. This result is a consequence of the milling process applied. Wet grinding with 96% ethanol favors the selective dissolution of Na^+ and Ca^{2+}, which in turn is favored by milling process that allows the particle size reduction. An alkaline medium of Na^+ and Ca^{2+} ions favors CO_2 capture, resulting in the formation of the detected carbonate phase [11].

With regard to the glasses compositions, intense diffraction peaks were observed for L25 Rf samples, with a relative decrease respect to the L30 Rf sample. Diffraction patterns of L25 Mf and L30 Mf samples showed not well defined diffraction peaks, so the crystalline phase was not detected as clearly as in L25 Rf and L30 Rf samples. For the rest of the compositions, diffraction peaks were even less intensive, being difficult to discern. But a distinctive characteristic was observed in L25 Rf and L30 Rf glasses, showing a greater amount of crystalline phase in comparison with L25 Mf and L30 Mf glasses, respectively.

Taking into account the above results, it is seen how Na and Ca ions are more available for those cases where a greater amount of surface crystalline carbonate is detected. In summary, L25 and L30 Rf glasses presented higher solubility than L25 and L30 Mf glasses, whereas L40 and L50 Rf were less soluble than L40 and L50 Mf.

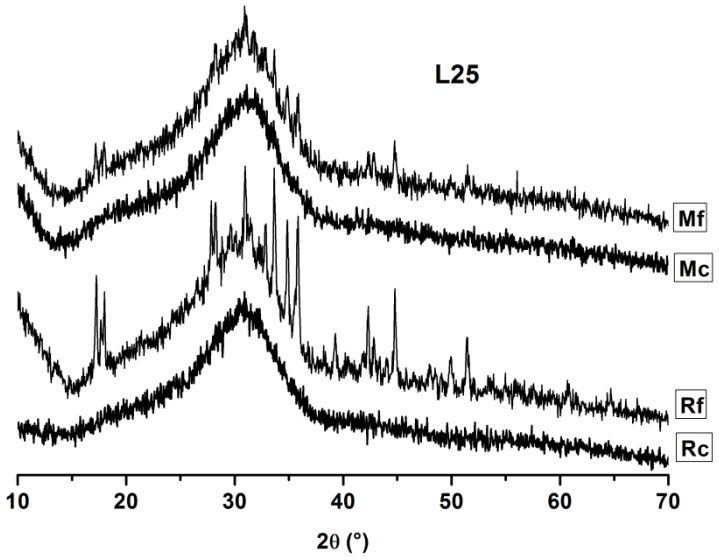

Figure 1. X-ray diffractograms of glasses L25 Mf, L25 Mc, L25 Rf and L25 Rc.

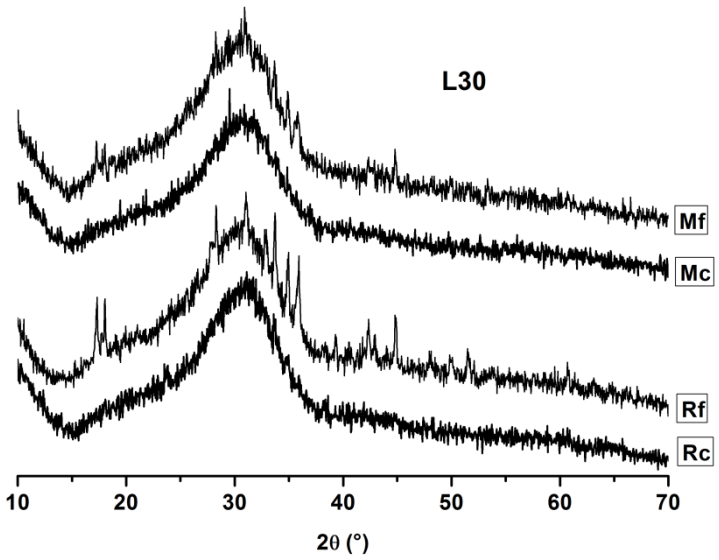

Figure 2. X-ray diffractograms of glasses L30 Mf, L30 Mc, L30 Rf and L30 Rc.

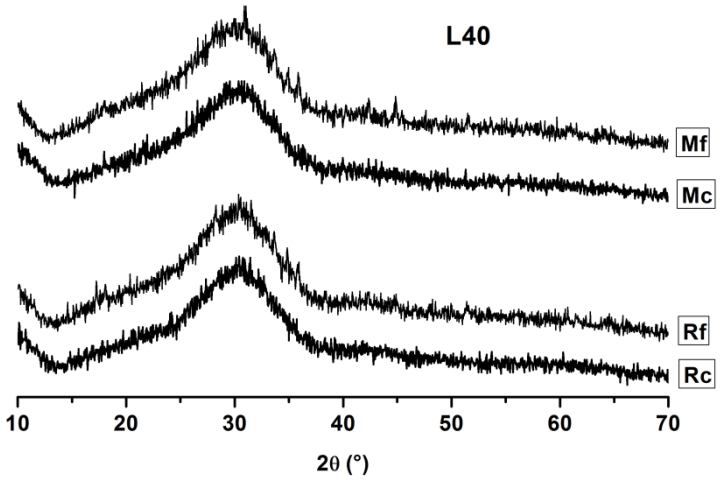

Figure 3. X-ray diffractograms of glasses L40 Mf, L40 Mc, L40 Rf and L40 Rc.

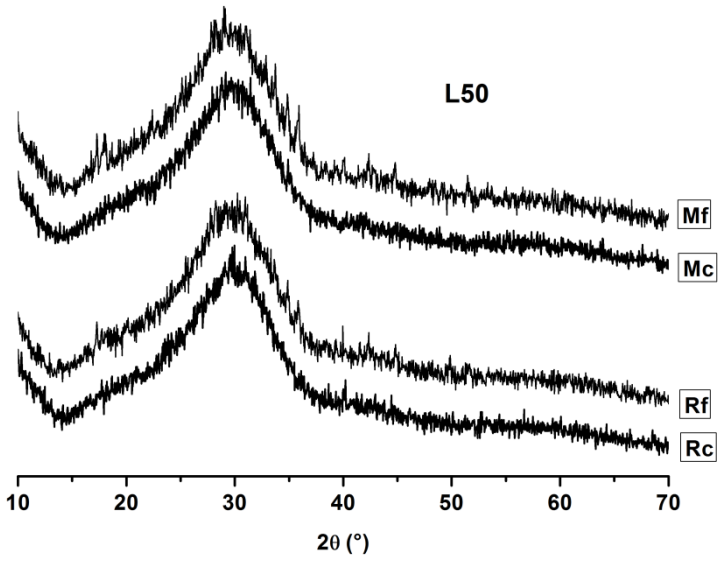

Figure 4. X-ray diffractograms of glasses L50 Mf, L50 Mc, L50 Rf and L50 Rc.

FT-IR

FT-IR spectra of the glasses showed bands located at 1150-1000 cm^{-1} ascribed to the Si-O-Si stretching vibrations, a shoulder at 920 cm^{-1} ascribed to the Si-O-(NBO)

stretching vibrations and a band located at 450-550 cm^{-1} corresponding to Si-O-Si symmetric vibrations [12]. A less intensive band centered at 600 cm^{-1} was assigned to the presence of symmetric P-O vibrations [13, 14]. Bands located at 700-800 cm^{-1} corresponded to symmetric Si-O-(NBO) stretching vibrations between tetrahedrons (Q3) [15](Figures 5-8).

Two bands located at 1420 and 1480 cm^{-1} confirmed the presence of CO_3^{2-} groups [16] in samples of the series L25, L30 and L40 (Figures 5, 6 and 7, respectively). Figure 8 shows L50 glasses spectra with a band located at 1420 cm^{-1}, whereas the band at 1480 cm^{-1} disappeared. With regard to the composition, a decreasing intensity of the carbonate bands was observed for the series L25-L50, which is related to the surface carbonate content. The bands mentioned before located at 1420 and 1480 cm^{-1} are due to the formation of surface carbonates with a defined crystalline structure, whereas the presence of a single band, as in L50 glass, is ascribed to the formation of poorly crystalline carbonates [16, 17].

In series L25-L30, it is noticed a difference respect to compositions, the band maximum at 700-800 cm^{-1} shifted from 775 to 750 cm^{-1}. This can be attributed to the increment of Al_2O_3 percentage that lead to progressive increase of Al-O vibrations, detected in the range of 730 cm^{-1} [18].

By comparing the spectra of the series L25 R and L30 R, a shift of the maximum of the band from 450-550 cm^{-1} to lower wavenumbers is observed after wet milling of the glasses produced by analytical grade reagents. This displacement is not perceivable in samples produced from natural minerals (L25 M and L30 M) after wet milling. In turn, this behavior is not as visible for L40 and L50 glasses, where no differences are observed among the spectra of the raw materials and after milling. This behavior has been reported in literature as a surface ions loss with the consequent formation of a silica rich layer [8].

In this sense, a shift of the band maximum from 650-750 cm^{-1} to higher wavenumber was also detected after the wet milling process in all samples. This band was associated to Al-O-Si stretching vibrations of tetrahedral linkages (700 cm^{-1}) overlapped with Si-O-Si stretching vibrations at 800 cm^{-1}. This displacement may be due to a relative intensity increase of the band corresponding to Si-O-Si vibrations as a consequence of the surface structural change after the milling process.

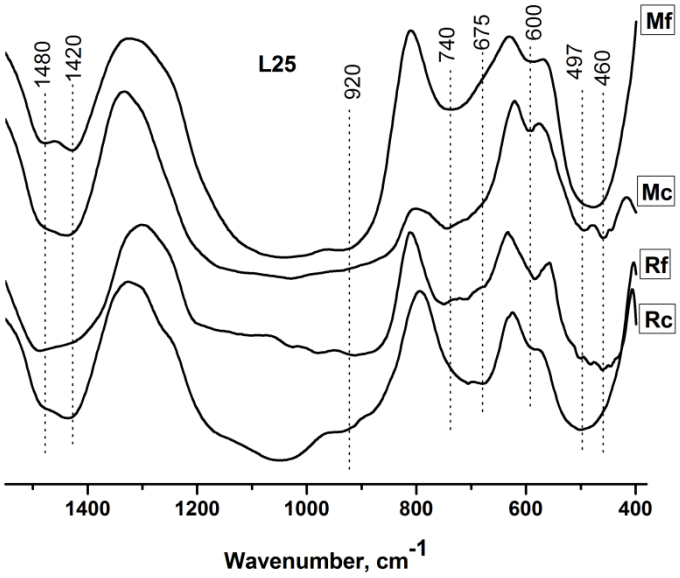

Figure 5. Infrared spectra of glasses L25 Mf, L25 Mc, L25 Rf and L25 Rc.

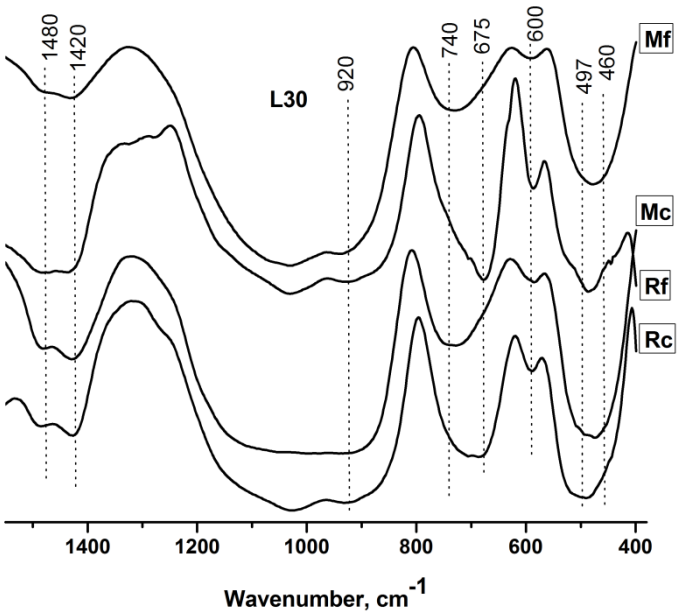

Figure 6. Infrared spectra of glasses L30 Mf, L30 Mc, L30 Rf and L30 Rc.

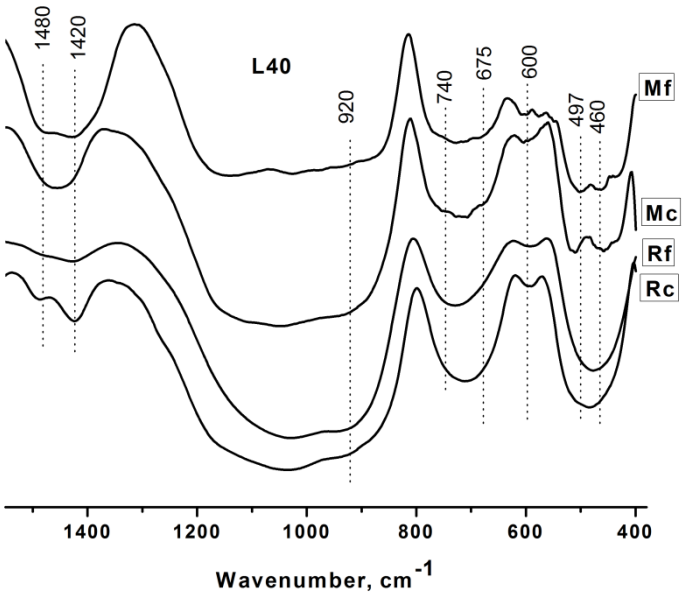

Figure 7. Infrared spectra of glasses L40 Mf, L40 Mc, L40 Rf and L40 Rc.

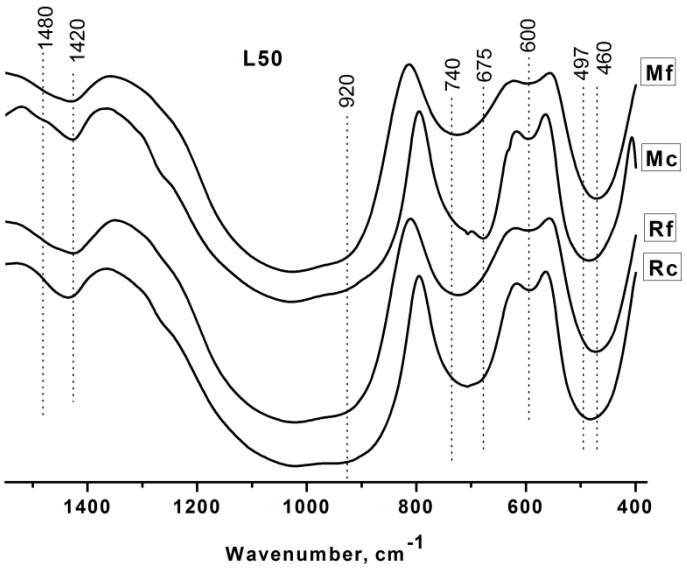

Figure 8. Infrared spectra of glasses L50 Mf, L50 Mc, L50 Rf and L50 Rc.

X-Ray Photoelectron Spectroscopy

Surface compositions values, determined by XPS, have been represented and normalized for each element as a function of the theoretical Leucite contents considered to produce glasses, excluding carbon and oxygen (Figures 9-14) A carbon layer is usually detected in glass surface after its production [19], so as oxygen could be a part of carbon compounds deposited on the surface [20].

After high energy wet milling (f) several changes such as a lower proportion of aluminum (Figure 10) in glasses L25, L30 and L40, in comparison with those dry milled (c), were observed. Aluminum surface concentrations in fine glasses (wet milled) trend to be closer to the detected values of coarse glasses until becoming similar in the series L25-L50. This same behavior was observed for silicon. In the case of phosphorus a similar behavior was observed, where the surface contents were closer between fine and coarse samples until become the same in L50. In this case, phosphorus content in wet milled glasses was higher than that observed in series L25-L40.

The Si 2*p* core level spectra of all prepared samples show a maximum at around 102.5 eV. The maximum of the peak was shifted to lower energies when the silicon content decreases [21]. In this work, silicon concentration was nearly constant.

The surface content of potassium on the wet milled samples remains lower than that observed for the dry milled samples in the entire range of compositions (Figure 9).

A singular behavior was observed for sodium and calcium. Their surface content in all compositional range of coarse glasses (c) was lower to that observed in bulk analysis (XRF). In turn, surface contents after wet milling were higher and, in some cases, even higher than those of the bulk. Sodium surface concentration was higher than those of the bulk in glasses L25 and L30, and the same behavior was found for calcium, except in the case of L30 Rf sample. This could be attributed to ethanol wet milling. As 96% ethanol was used, the remaining water could have selectively dissolved alkali ions which were then concentrated over the surface as a part of carbonates compounds. The composition L40 and L50 showed an opposite trend. These results are in agreement with XRD and FTIR data, where diffraction lines and vibration frequencies of carbonates were detected.

Broadly, several differences for high energy milled samples (f) were found depending on the raw materials used to produce glasses. As an illustrative example, greater amounts of phosphorus and calcium were detected in samples L25 Mf and L30 Mf in comparison with samples L25 Rf and L30 Rf. In samples L25 Mf and L30 Mf, a minor aluminum content was found than that in L25 Rf and L30 Rf, remaining as a constant in the rest of compositions. Considerable differences were also noticed for the rest of the elements in comparison with the raw materials, although the behavior is oscillatory without noticing any clear trend.

The C 1*s* core level spectrum showed two peaks associated to different chemical environments. In all the studied samples a peak around 285 eV, associated to C-C

linkages, mainly from adventitious carbon [19], and another one at about 289 eV associated to carbonates, are present [22, 23](Figure 15). However, the relative intensities of both peaks vary depending on the applied milling process. In general, an increase of the relative intensity of the peak located at around 289 eV was observed in wet milled glasses with respect to dry milled ones. This implies that the wet milling lead to a surface enrichment with carbonate. Other observed trend is the decreasing intensity related to the peak located at 289 eV in the series L25-L50, for wet and dry milled samples. This implies a decrease in the carbonate content until its disappearance in dry milled glasses L40 and L50 (Figure 15). Surface Carbon content from carbonate (Figure 16) showed a similar trend than that of relative carbon chemical environment. Results showed in Figure 16 indicate that carbonate quantities do not differ significantly between samples made from different raw material, but they do differ in crystallinity.

Briefly, in accordance with all the characterization techniques results, it was found that glasses with 25 and 30 wt. % of theoretical Leucite content made from analytical grade raw materials showed a significant surface and structural differences with respect to glasses of the same compositions made from natural minerals.

The AlKLL signal can be used to distinguish between tetrahedral and octahedral coordination of aluminum [24]. With respect to the detected coordination of Al (Figure 17), an ascendant trend related to the octahedral aluminum is observed in the order L25-L50, coinciding with the increasing amount of Al_2O_3 into the composition. It is known that aluminum reduce degradation rate of glasses, but an increase in AlO_6 units may increase degradation rate because of defects induced in the glass network [25]; so a higher content of octahedral coordinated aluminum could be beneficial to bioactivity.

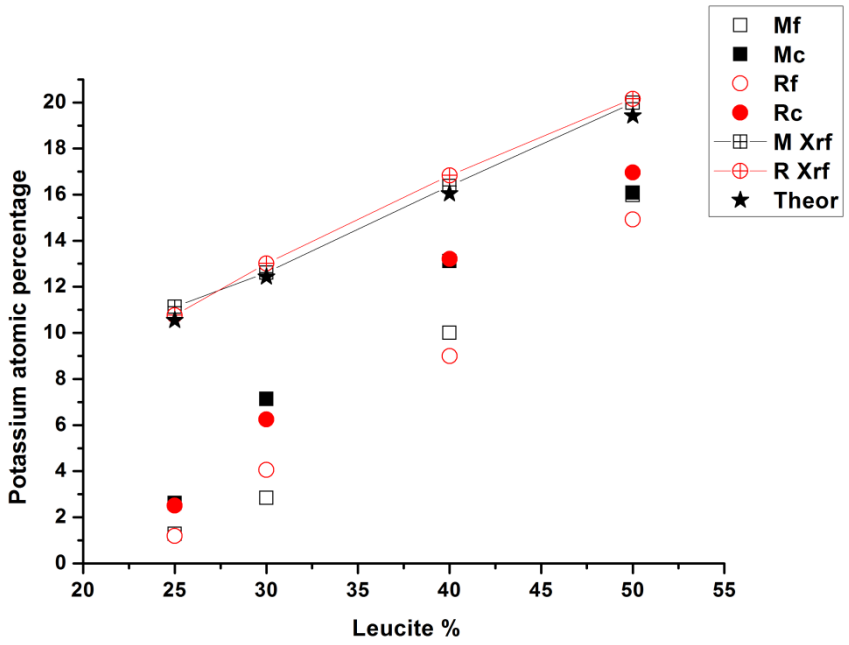

Figure 9. Normalized Surface concentration of K measured by XPS analysis as a function of glass composition, compared with the corresponding theoretical concentration and bulk analysis (XRF).

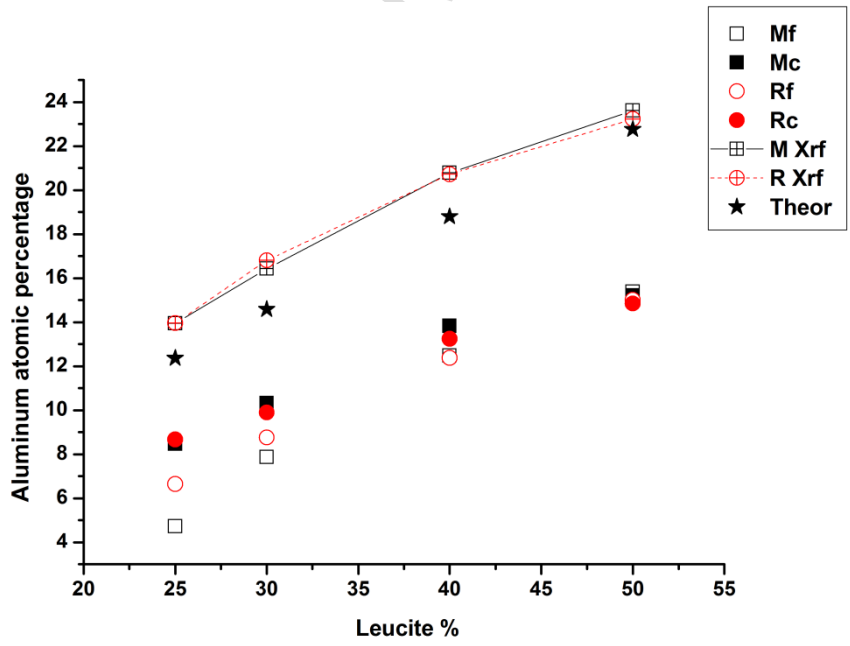

Figure 10. Normalized Surface concentration of Al measured by XPS analysis as a function of glass composition, compared with the corresponding theoretical concentration and bulk analysis (XRF).

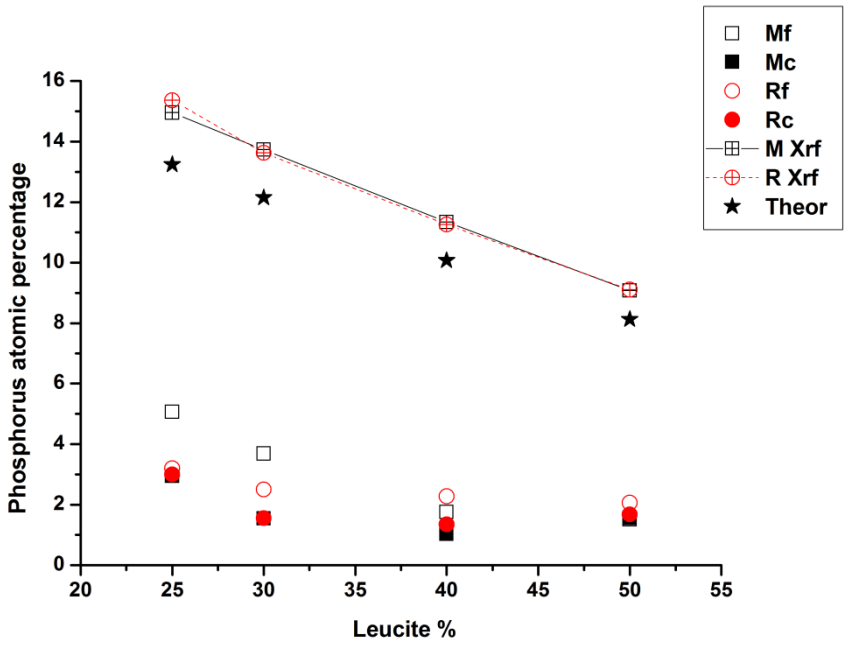

Figure 11. Normalized Surface concentration of P measured by XPS analysis as a function of glass composition, compared with the corresponding theoretical concentration and bulk analysis (XRF).

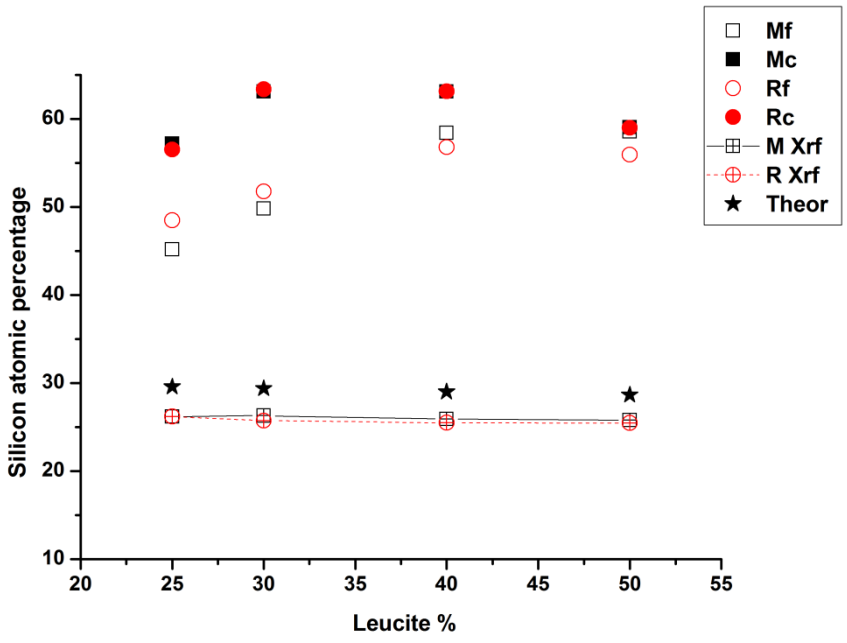

Figure 12. Normalized Surface concentration of Si measured by XPS analysis as a function of glass composition, compared with the corresponding theoretical concentration and bulk analysis (XRF).

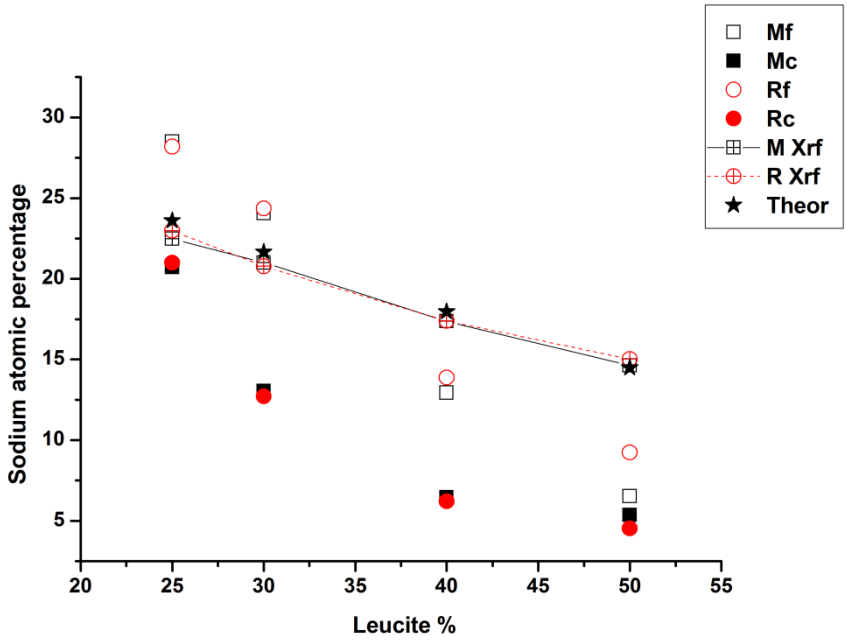

Figure 13. Normalized Surface concentration of Na measured by XPS analysis as a function of glass composition, compared with the corresponding theoretical concentration and bulk analysis (XRF).

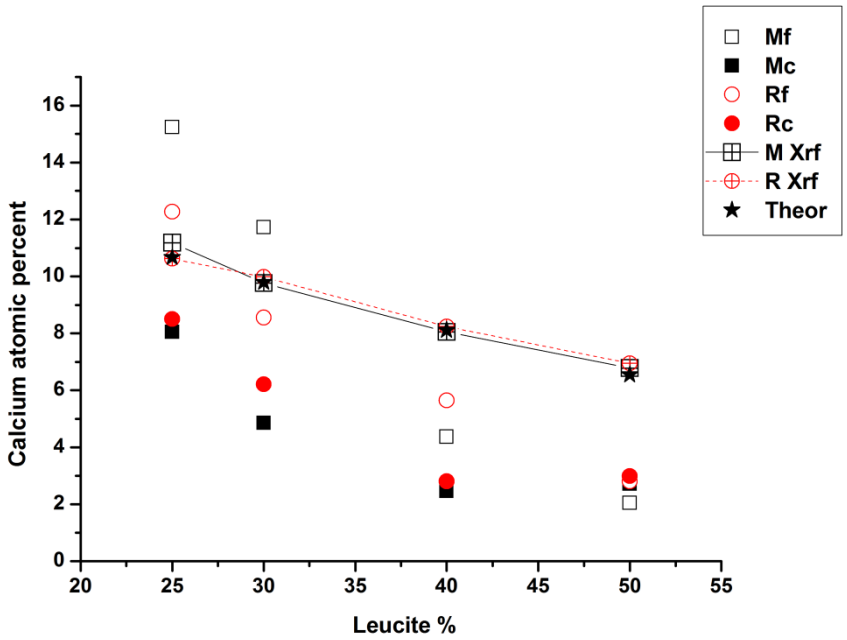

Figure 14. Normalized Surface concentration of Ca measured by XPS analysis as a function of glass composition, compared with the corresponding theoretical concentration and bulk analysis (XRF).

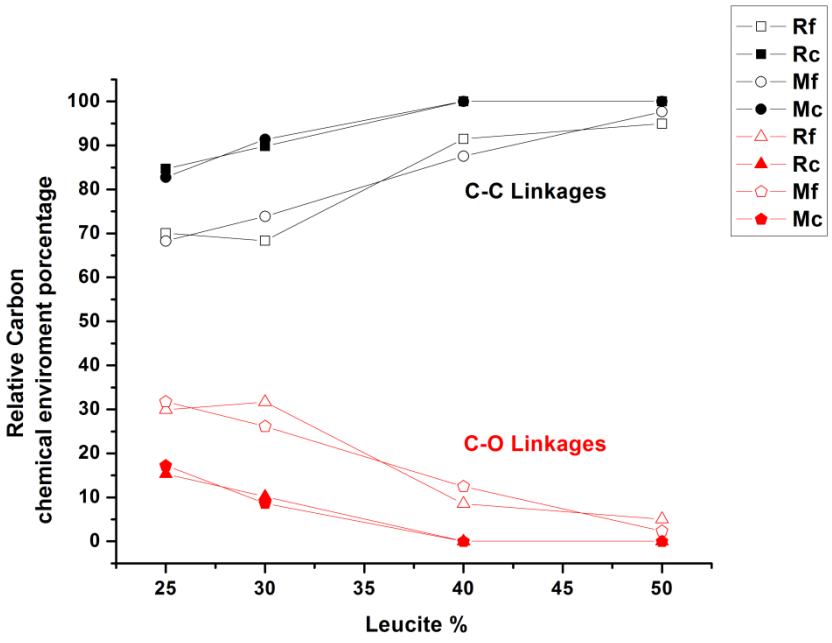

Figure 15. Carbon chemical environment (C-C and C-O) as a function of glass composition.

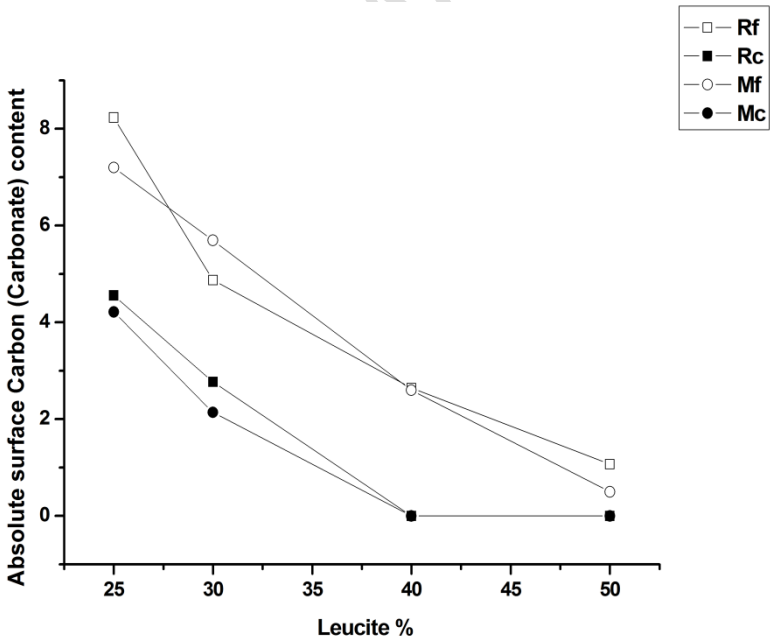

Figure 16. Surface Carbon content due to Carbonate formation.

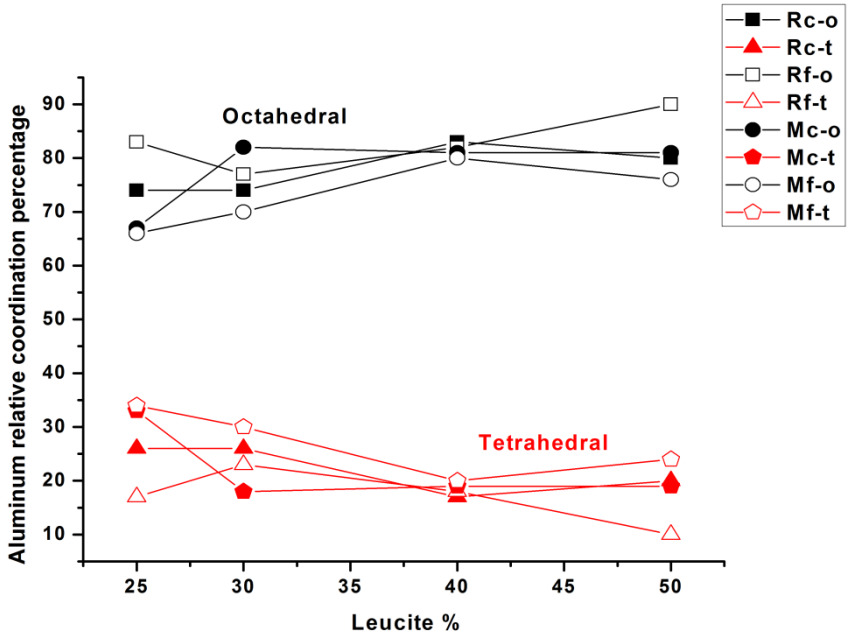

Figure 17. Aluminum coordination as a function of glass composition.

Discussion

In general, differences were observed regarding both the degree of milling and the composition of glasses. The wet milling process of glasses L25 R and L30 R led to the formation of a surface layer of sodium calcium carbonate (Pirssonite). Something similar happened with samples L25 M and L30 M after wet milling. The amount of surface crystalline carbonate present on glass L25 Rf and L30 Rf was greater than that detected on the surfaces of L25 Mf and L30 Mf. However, the quantities of carbonate present in the four mentioned samples would be similar according to the results obtained by FTIR and XPS, and the largest differences were found in the carbonates crystallinity.

It is possible that this difference appeared due to a difference in the dissolution rate of glasses. Although the amount of developed carbonate was comparable, it is possible that the release of ions from glasses L25 Rf and L30 Rf to the environment occurred in a lower time lapse, so, since the total time of the complete process (wet milling and ethanol drying) were the same in all cases, these samples (L25 Rf and L30 Rf) have

had a longer time to develop as many crystalline carbonate. The difference in the rate of dissolution may be due to that, even though all the precautions were taken so as to obtain homogeneous glasses, it is possible that L25 Mf and L30 Mf glasses have a different microstructure that L25 Rf L30 Rf. The use of feldspar could have caused local concentrations of K_2O, Al_2O_3, and SiO_2, the major feldspar components, because it is well known that these three components substantially increase the viscosity of the glass. That possible local concentration could have generated a lack of homogenization in those areas. It is also known that these aforementioned components increase the corrosion resistance of glasses. In summary, those areas with a greater local concentration of the oxides mentioned would be more resistant to dissolution in glasses L25 Mf and L30 Mf, hence its lower global dissolution rate with regard to glasses L25 Rf and L30 Rf, which would have reached a greater homogenization, probably because the contribution of the constituent oxides was done in an individual way (each raw material used only brought a single oxide), reaching a greater dispersion of those components.

For the rest of the compositions (L40 and L50) no significant differences were found in surface contents of carbonate with respect to the raw materials used after the wet milling. In all cases (L40 Rf, L50 Rf, L40 Mf and L50 Mf) carbonates developed did not possess crystalline structure, so it may be said that their behavior toward the dissolution were similar. With respect to these samples, it is possible that the degree of homogeneity achieved for this range of compositions, regardless of the raw materials used, were similar in all of them. The latter may have occurred due to the content of the oxides K_2O, Al_2O_3 and SiO_2 was similar to the rest of the components for which the same dispersion of components would be reached if the oxides were added independently or through minerals such as feldspar that contributes to the three oxides simultaneously.

With regard to the dry milling, only an amorphous carbonate layer was developed on glasses L25 Mc, L30 Mc, L25 Rc and L30 Rc, while adventitious carbon was only found in the rest of the compositions (L40 Mc, L50 Mc, L40 Rc and L50 Rc). Due to the higher reactivity of glasses L25 Mc, L30 Mc, L25 Rc and L30 Rc, carbonate formation occurred due to surface corrosion caused by environmental water. Corrosion was less significant than in the case of wet milled specimens due to the conditions difference and to the particle size, which leaves a smaller surface area exposed.

Conclusions

Sodium and calcium ions were dissolved from the surface of the prepared glasses in greater or lesser extent after the wet milling with ethanol. This release increases the pH allowing the capture of atmospheric CO_2 in the liquid medium. The ions release was directly dependent on the glasses compositions and the subsequent formation of surface carbonate. Carbonate content increases with decreasing in theoretical Leucite content (in the order L50-L25).

Glass changes depend on both composition and starting raw materials. Glasses with low theoretical Leucite content (L25 and L30) produced from analytical grade reagents showed a higher dissolution rate of alkali ions after wet milling (L25 Rf and L30 Rf) with respect to the same glasses compositions made from natural raw materials (L25 Mf and L30 Mf). The differences in dissolution kinetics allowed glasses L25 Rf and L30 Rf to develope major quantities of crystalline carbonate formation (Pirssonite) with respect to L25 Mf and L30 Mf. Nevertheless, the total carbonate amounts (crystalline and amorphous) were essentially the same regardless the raw materials origin. Dissolution rate differences within the same compositions regarding different raw materials were referred to a different degree of homogenization of glasses.

L40 and L50 glasses (40 and 50 % of theoretical Leucite content) developed surface carbonates with an amorphous structure after wet milling. Glasses of L50 composition

did not present substantial differences with respect to the raw materials as well as with respect to the applied milling process.

Acknowledgements

The authors thanks to CONICET (*National Scientific and Technical Research Council*) for its financial support (PIP 0248), MINECO project CTQ2015-68951-C3-3-R of Spain and FEDER Funds and Jose Ortiga for his important technical assistance.

Reference

[1] J.R. Jones, Acta biomaterialia, 9 (2013) 4457-4486.

[2] M. Manda, O.-M. Goudouri, L. Papadopoulou, N. Kantiranis, D. Christofilos, K. Triantafyllidis, K.M. Paraskevopoulos, P. Koidis, Ceramics International, 38 (2012) 5585-5596.

[3] O.M. Goudouri, E. Kontonasaki, L. Papadopoulou, N. Kantiranis, N. Lazaridis, K. Chrissafis, X. Chatzistavrou, P. Koidis, K. Paraskevopoulos, Materials Chemistry and Physics, 145 (2014) 125-134.

[4] F.M. Stábile, C. Volzone, Materials Research, 17 (2014) 1031-1038.

[5] M.J. Cattell, T.C. Chadwick, J.C. Knowles, R.L. Clarke, D.Y. Samarawickrama, dental materials, 22 (2006) 925-933.

[6] W. Höland, M. Frank, V. Rheinberger, Journal of non-crystalline solids, 180 (1995) 292-307.

[7] E. El-Meliegy, R. van Noort, Glasses and Glass Ceramics for Medical Applications, Springer Science & Business Media, 2011.

[8] S. Romeis, A. Hoppe, C. Eisermann, N. Schneider, A.R. Boccaccini, J. Schmidt, W. Peukert, Journal of the American Ceramic Society, 97 (2014) 150-156.

[9] S. Abdollahi, A.C.C. Ma, M. Cerruti, Langmuir, 29 (2013) 1466-1474.

[10] F.M. John, F.S. William, E.S. Peter, D. Kenneth, Perkin-Elmer Corporation Physical Electronics Division, (1992).

[11] M. Cerruti, C. Morterra, Langmuir, 20 (2004) 6382-6388.

[12] O. Peitl, E. Dutra Zanotto, L.L. Hench, Journal of Non-Crystalline Solids, 292 (2001) 115-126.

[13] N. Nabian, M. Jahanshahi, S.M. Rabiee, Journal of Molecular Structure, 998 (2011) 37-41.

[14] L. Lefebvre, J. Chevalier, L. Gremillard, R. Zenati, G. Thollet, D. Bernache-Assolant, A. Govin, Acta Materialia, 55 (2007) 3305-3313.

[15] F.H. ElBatal, A. ElKheshen, Materials Chemistry and Physics, 110 (2008) 352-362.

[16] M. Cerruti, D. Greenspan, K. Powers, Biomaterials, 26 (2005) 1665-1674.

[17] F.A. Miller, C.H. Wilkins, Analytical Chemistry, 24 (1952) 1253-1294.

[18] D. Zhao, W. Huang, M.N. Rahaman, D.E. Day, D. Wang, Acta biomaterialia, 5 (2009) 1265-1273.

[19] Q. Chen, K. Rezwan, D. Armitage, S. Nazhat, A. Boccaccini, Journal of Materials Science: Materials in Medicine, 17 (2006) 979-987.

[20] M.S. Bahniuk, H. Pirayesh, H.D. Singh, J.A. Nychka, L.D. Unsworth, Biointerphases, 7 (2012) 41.

[21] J. Serra, P. González, S. Liste, C. Serra, S. Chiussi, B. León, M. Pérez-Amor, H. Ylänen, M. Hupa, Journal of Non-Crystalline Solids, 332 (2003) 20-27.

[22] J. Santos, L. Jha, F. Monteiro, Journal of Materials Science: Materials in Medicine, 7 (1996) 181-185.

[23] J.T. Verhoeven, H. Van Doveren, Surface Science, 123 (1982) 369-383.

[24] M. Gómez-Cazalilla, J. Mérida-Robles, A. Gurbani, E. Rodríguez-Castellón, A. Jiménez-López, Journal of Solid State Chemistry, 180 (2007) 1130-1140.

[25] G.J. Mohini, N. Krishnamacharyulu, G. Sahaya Baskaran, P.V. Rao, N. Veeraiah, Applied Surface Science, 287 (2013) 46-53.

Highlights

- Four glass compositions were produced from raw materials of different origins.
- Glass compositions have different theoretical Leucite/Bioglass 45S5 ratios.
- Glasses with 25 and 30 wt. % of Leucite showed higher dissolution after wet milling.
- Pirssonite was found on the surface of glasses with 25 and 30 wt. % of Leucite.
- Less carbonate formation was found in glasses produced from minerals.